THE JOURNAL OF PHYSICAL CHEMISTRY LETTERS
A JOURNAL OF THE AMERICAN CHEMICAL SOCIETY

pubs.acs.org/JPCL

Letter

Picosecond Charge Localization Dynamics in $CH_3NH_3PbI_3$ Perovskite Probed by Infrared-Activated Vibrations

Klara Stallhofer, Matthias Nuber, Daniele Cortecchia, Annalisa Bruno, Reinhard Kienberger, Felix Deschler, Cesare Soci,* and Hristo Iglev*

Cite This: *J. Phys. Chem. Lett.* 2021, 12, 4428–4433

Read Online

ACCESS | Metrics & More | Article Recommendations | Supporting Information

ABSTRACT: Hybrid metal halide perovskites exhibit well-defined semiconducting properties and efficient optoelectronic performance considering their soft crystal structure and low-energy lattice motions. The response of such a crystal lattice to light-induced charges is a fundamental question, for which experimental insight into ultrafast time scales is still sought. Here, we use infrared-activated vibrations (IRAV) of the organic components within the hybrid perovskite lattice as a sensitive probe for local structural reorganizations after photoexcitation, with femtosecond resolution. We find that the IRAV signal response shows a delayed rise of about 3 ps and subsequent decay of pronounced monomolecular character, distinguishing it from absorption associated with free carriers. We interpret our results as a two-step carrier localization process. Initially, carriers localize transiently in local energy minima formed by lattice fluctuations. A subpopulation of these can then fall into deeper trapped states over picoseconds, likely due to local reorganization of the organic molecules surrounding the carriers.

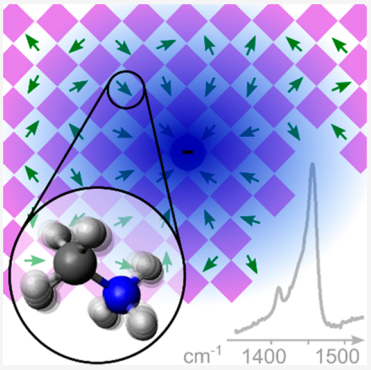

The promise of efficient solar cells based on metal halide perovskites, which can be versatilely and inexpensively processed by low-temperature solution[1] or vacuum based processes and scaled to large dimensions,[2,3] has drawn considerable attention over the past few years. Among the materials investigated in this context, $CH_3NH_3PbI_3$ ($MAPbI_3$) is probably the most widely studied and can be considered a standard in this field. It offers highly desirable optical properties[4] as well as a long charge carrier lifetime and diffusion lengths.[5] The soft and deformable polar lattice of $MAPbI_3$ implies significant coupling between electronic and vibrational degrees of freedom and is distorted in the presence of a charge. Such structural deformations have been associated with the formation of large polarons,[6−9] which, in turn, have been associated with the formation of long-term photoinduced degradation processes by halide separation.[10] The role of the methylammonium (MA) cations in polaron formation, freely rotating within the inorganic scaffold at room temperature, has been a subject of debate.[11−13] A consensus regarding the question whether the organic cations are essential to polaron formation has not yet been reached.[14−16] Nonetheless, the dipole moment of the cations should, in any case, render them sensitive to the presence of a charge. Because the organic cations can interact with the inorganic sublattice via interactions between ions and between ions and dipoles, as well as hydrogen bonding, structural deformations will affect both constituents.

Time-resolved measurements in the mid-infrared spectral range offer the opportunity to observe spectrally broad absorption features of electronic origin and sharp absorption peaks associated with vibrational modes of the organic cations simultaneously.[17−21] The latter appear in the form of infrared-activated vibrations (IRAVs) in the presence of a charge. The concept of IRAVs has been introduced in the field of conjugated polymers, where they appear as intense absorption peaks in the electronic excited state.[22−24] Because of the sensitivity of the underlying molecular vibrations of the MA cations toward structural properties, these IRAVs can be employed as indicators of processes, which are accompanied by deformations of the perovskite structure.[25]

Pronounced structural distortions are involved in the process of charge localization, which are reflected in the properties of the IRAVs. Charge localization has been shown to be induced via dynamic disorder evoked by the mechanically soft lattice as well as the MA molecules.[26−28] A two-step localization process has recently been inferred from calculations.[29] Initially, the excess charge is localized by local thermal fluctuations of the structure. In a second step, the charge affects its surroundings, leading to further distortion of the inorganic lattice and reorientation of MA cations, thus completing the localization process. Following a similar line of thought, initial localization has also been suggested to be triggered by the disordered

Received: March 23, 2021
Accepted: May 4, 2021
Published: May 5, 2021

https://doi.org/10.1021/acs.jpclett.1c00935
J. Phys. Chem. Lett. 2021, 12, 4428–4433

dipolar field of organic cations and then further stabilized by distortions of the inorganic sublattice.[26] Furthermore, by comparison of the properties of hybrid perovskites to those of all-inorganic perovskites, it has been shown that localized polar fluctuations are a general feature of lead halide perovskites, and the dipolar organic cation is no prerequisite for their occurrence.[30] In accordance with these observations, ultrafast electron diffraction measurements reported the evolution of light-enhanced local disorder of the inorganic lattice on a picosecond time scale.[31] A comparable time scale for structural changes of the inorganic sublattice has also been derived from the observation of long-lived anisotropy in several perovskites.[32] This effect is ascribed to dynamically fluctuating deformations confined to small regions of the lattice, which spontaneously lead to localized polarized distortions on a time scale of picoseconds.

In this Letter, we study the interplay between charge carrier recombination dynamics and the structural changes induced in $MAPbI_3$ perovskite by transient mid-IR spectroscopy. We propose that the IRAVs observed in the mid-IR spectrum associated with vibrational modes of the MA cations represent a sensitive probe for structural reorganization processes upon electronic excitation and reflect the localization of charge carriers on a time scale of a few picoseconds.

The absorption peaks in the infrared spectrum of the $MAPbI_3$ thin film (see Figure 1a) between 1000 and 3500 cm^{-1} can be attributed to the vibrations of the organic MA cations (experimental details on steady-state spectroscopy can be found in the Supporting Information). The NH_3^+ stretching vibrational modes are found around 3150 cm^{-1}, while the bending vibrations of the molecule lie between 1390 and 1630 cm^{-1} (see Figure 1b). Here, the NH_3^+ symmetric bending vibration at 1468 cm^{-1} is the most prominent one, flanked by the asymmetric CH_3 bending mode at 1421 cm^{-1} and the asymmetric NH_3^+ bending mode at 1578 cm^{-1}. The ground-state absorption of the former two vibrations is included in the spectral range covered by the probe beam in the time-resolved measurements, where the 500 nm pump beam results in above-band-gap electronic excitation, as indicated in the visible spectrum shown in Figure 1c.

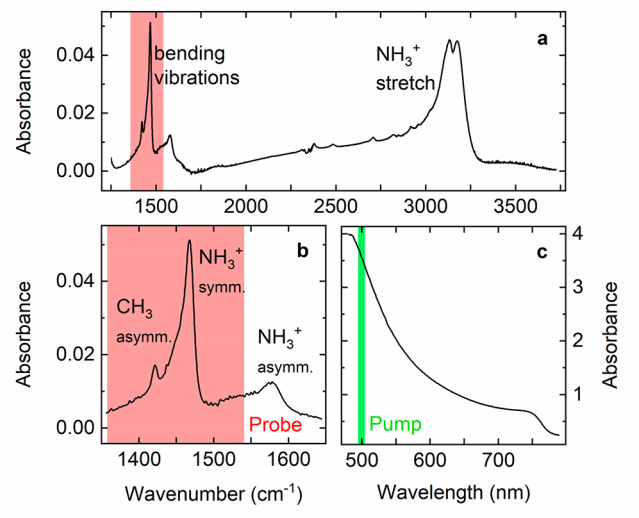

Figure 1. Steady-state spectra of $MAPbI_3$ thin film. (a) FTIR spectrum with spectral range covered by the probe beam in the time-resolved measurements marked in red. (b) Enlarged view of the methylammonium bending vibrations in (a). (c) Visible spectrum with spectral position of the pump beam at 500 nm.

Transient spectra show a broad absorption covering the whole spectral range investigated, overlaid with sharper absorption peaks centered at 1475 and 1400 cm^{-1} (see Figure 2 for the spectra at an initial charge carrier density of ~5.4 × 10^{19} cm^{-3}; spectra for more intense pumping can be found in Figure S1). Both features were also observed in mid-IR measurements on the nanosecond time scale[14,19−21] and with quasi-steady-state measurements covering a wider spectral range.[25] In these experiments, a broad absorption line shape increasing toward lower energy was also present, peaking around 1200 cm^{-1} and followed by a sharp dip in absorption toward lower frequencies. This absorption was attributed to photoexcitation of self-trapped charge carriers, i.e., polarons, since the absorption edge disagrees with identifying the background as pure Drude absorption of free carriers. It could be reproduced by a large polaron model.[20,33]

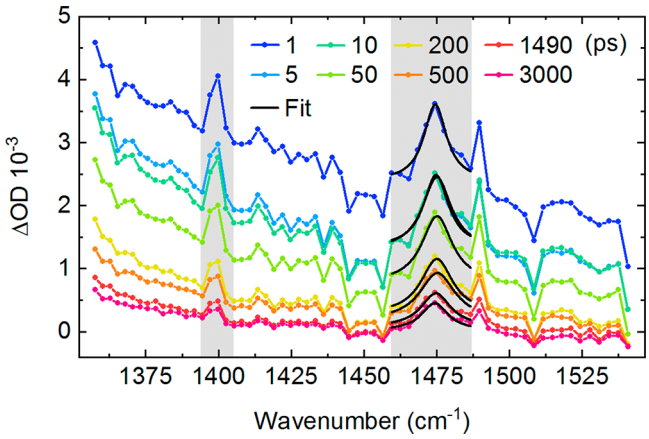

Figure 2. Transient IR absorption spectra measured at indicated delay times after optical excitation at 500 nm with an initial excitation density of ~5.4 × 10^{19} cm^{-3}. IRAV modes associated with CH_3 and NH_3^+ bending modes are marked in gray.

In analogy to similar observations in conjugated polymers,[34] the sharp absorption features atop of the broad background are identified as IRAVs of enhanced amplitude induced in the presence of a charge, which can be associated with vibrational modes in the ground state. It has been previously demonstrated that in polymers they arise due to structural reorganization around the excess charge, which leads to Raman modes becoming IR-active.[22,35] In $MAPbI_3$, the ground-state vibrations associated with the observed IRAV modes are the symmetric NH_3^+ bending mode for the absorption at 1475 cm^{-1} and the asymmetric CH_3 bending mode in the case of the smaller peak at 1400 cm^{-1}. The former is blue-shifted by 7 cm^{-1} with respect to its ground-state absorption, while the latter shows a red-shift by 21 cm^{-1}.

Several possible explanations for the IRAV in the excited electronic state are worth considering. All of them are based on interaction between the photoinduced charge and the MA cation. The observed frequency shift might be due electrostatic interaction leading to a redistribution of charge density on the molecule, sometimes also termed the vibrational Stark effect,[18,36] or be mediated by a change in hydrogen bond strength between the MA and the inorganic lattice.[37−39] According to the empirical Badger's rule,[40] a change in

https://doi.org/10.1021/acs.jpclett.1c00935
J. Phys. Chem. Lett. 2021, 12, 4428−4433

bonding strength is reflected in a frequency shift of the associated vibrational mode. Both mechanisms would account correctly for the observed frequency shift in opposite directions of the IRAV associated with NH_3^+ and CH_3 as compared to their respective absorption in the ground state.[38] For a more detailed discussion of the physical phenomena that might contribute to the interaction between the MA and the photoexcited charge, we refer the reader to the Supporting Information (see page S4).

The origin of intensified IR bands in the electronically excited state has also been attributed to the modulation of charge distribution by vibrational motion[23,24] or to the mixing of low-lying electronic and vibrational transitions.[41] Our measurements do not clearly speak in favor of one of the above processes. It seems likely that a combination of the mechanisms presented is responsible for the formation of the IRAV.

While associated with specific molecular vibrations, IRAVs need to be clearly distinguished from the excited-state absorption (ESA) upon vibrational excitation. The ESA manifests itself in absorption that is red-shifted in comparison with the respective vibrational mode in the ground state due to anharmonicity of the vibrational potential and is accompanied by bleaching of the ground state (GSB). No such bleaching is observed here.

To exclude a pump-induced temperature rise as the main cause of the observed sharp absorption features, a series of FTIR measurements were conducted to investigate temperature-induced absorption changes. Neither the derivative-like shape nor the position of the spectral feature associated with temperature change resembles the IRAV absorption in the electronic excited state (see Figure S2). Thus, there are furthermore no indications of cooling of thermalized hot carriers with an effective temperature above that of the surrounding lattice, which would also result in temperature-related spectral changes.

For short delay times up to 0.5 ps, background spectral dynamics resemble a shift toward higher energies or a broadening of the underlying absorption profile that is not clearly separable from dispersion effects or possible coherent interaction between pump and probe at earliest times. After 0.5 ps, a uniform decay without significant spectral changes to the background is observed (see Figure 2). With increasing excitation intensity, the maximum amplitude at 1.5 ps increases proportionately (see Figure S3), and the decay is accelerated considerably (see Figure 3a). We extract kinetics at selected positions in the transient IR absorption (see Figure 3). A free carrier recombination model,[42,43] including a bimolecular and a monomolecular component, does not reproduce the decay dynamics of the charge carrier density n with time t to a satisfactory degree over the whole time window observed. The initial faster decay dominated by bimolecular processes and the slower process usually attributed to monomolecular recombination cannot be replicated at the same time: the contribution of either one of the processes is always underestimated. To allow for variation in the relative contribution of both processes, we adopt a model with independent bimolecular and monomolecular contributions, implying a decaying charge carrier population with an additional contribution that follows dominantly monomolecular recombination, as discussed below:

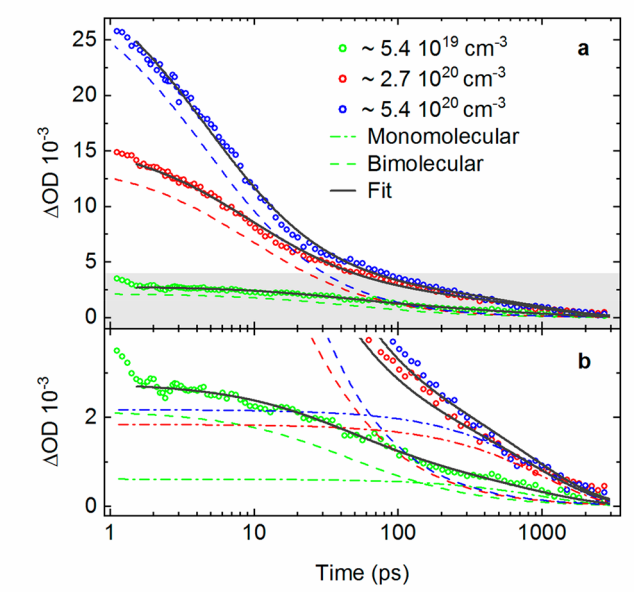

Figure 3. Recombination dynamics of the absorption background at 1390 cm^{-1} for different excitation fluences. (a) Experimental data and global fit curves including a bimolecular and a monomolecular recombination term. The bimolecular component is indicated by dashed lines. (b) Enlarged view of the area marked in gray in (a) with the monomolecular contribution represented by the dash-dotted curve.

$$n(t) = an_0 e^{-t/\tau_1} + b\frac{n_0}{n_0\gamma_2 t + 1}$$

A global fit for all three excitation intensities with bimolecular recombination coefficient γ_2 and the monomolecular decay time τ_1 as shared parameters is employed. The experimental parameters a and b are allowed to vary with excitation intensity (for fit parameters see Table S1). They include the optical cross section, which is independent of carrier density and accounts for deviations from the standard free carrier recombination model. The initial charge carrier density n_0, as estimated from the employed excitation intensity and the absorption properties of the perovskite (see Supporting Information), is set as a fixed parameter. The fit results in $\gamma_2 = 4 \times 10^{-10}$ cm^3/s and $\tau_1 = 1$ ns. Bimolecular recombination coefficients for $MAPbI_3$, as determined based on the standard free carrier recombination model, commonly are on the order of 10^{-9}–10^{-10} cm^3/s for the tetragonal phase at room temperature.[44−49]

The amplitude increase of the monomolecular component shows a saturation behavior at higher initial charge carrier densities (see Figure 3b). While bimolecular recombination dominates at shorter delay times, dynamics from 100 ps onward are mostly determined by the monomolecular contribution, according to the development of their fitted amplitudes with time.

Turning to the evolution of IRAV dynamics, we focus on the mode associated with the NH_3^+ vibration, since its broader spectral width allows a clearer assessment of the peak compared to the CH_3 IRAV, which is mostly defined by only two pixels. The determined dynamics of both modes are comparable (see Figure S4). To follow the NH_3^+ IRAV peak dynamics, a Lorentzian is fit to the peak at each individual time delay (see Figure 2), and its area is taken as a measure of

https://doi.org/10.1021/acs.jpclett.1c00935
J. Phys. Chem. Lett. 2021, 12, 4428−4433

oscillator strength. An increase within the first few picoseconds is followed by recombination over hundreds of picoseconds (see Figure 4). The maximum area of the IRAV mode is not

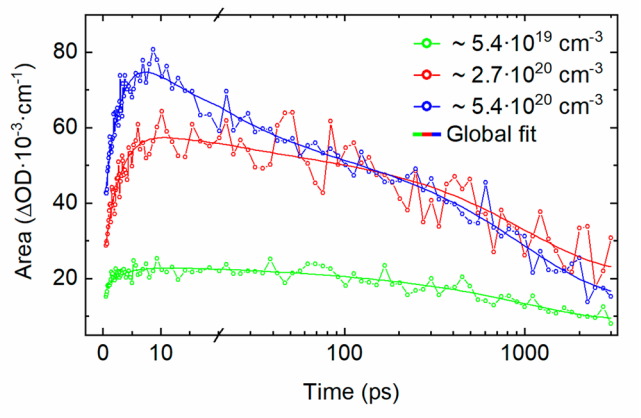

Figure 4. Temporal evolution of NH_3^+ IRAV peak area for different initial charge carrier densities together with the fitting curves.

proportional to excitation intensity but shows pronounced saturation effects. The initial rise distinguishes the IRAV mode dynamics clearly from the underlying broad background absorption at short times. The IRAV signal increase is characterized by a time constant of 3 ps.

Furthermore, the dynamics of the IRAV mode differ not only in the initial rise, which is not found in the background dynamics, but also in their decay. Two recombination processes occurring on distinct time scales are found for the IRAV, which are indeed similar to the two components identified in the background. For the fit curves shown in Figure 4, the decay rates are fixed to the same values as in Figure 3, namely $\gamma_2 = 4 \times 10^{-10}$ cm^3/s and $\tau_1 = 1$ ns. Thereby, we follow the findings for the nanosecond time scale, where the broad polaron absorption and the NH_3^+ peak show a concomitant decay.[21] However, there is a stark difference in the relative amplitudes of bimolecular and monomolecular components. For the IRAV dynamics the ratio between both components is 6−15 times smaller than for the background (see Table S2 for fit function and parameters).

The monomolecular contribution observed for the IRAV dynamics and the one in the background absorption show a similar dependence on excitation density. The contribution to the dynamics of the NH_3^+ peak area increases by a factor of 2.5 for an increase in initial charge carrier density from about 5.4×10^{19} to 2.7×10^{20} cm^{-3} and by a factor of 1.2 from 2.7×10^{20} to 5.4×10^{20} cm^{-3}. At the same time, the amplitude of the monomolecular decay component of the background absorption increases 3.0 and 1.2 times, respectively. The similar saturation effect with regard to initial charge density in combination with the shared relaxation constant gives evidence that both monomolecular processes are interconnected. Monomolecular recombination dominates the time period relevant for efficient charge separation in hybrid perovskite solar cells.

The different overall temporal dynamics of background and IRAV modes seems to indicate the presence of two different charge carrier species: one showing predominantly bimolecular recombination and contributing mainly to the background absorption and the other recombining primarily via a monomolecular process and dominating the IRAV response. As substantiated by the significant bimolecular contribution that dominates at high excitation densities, the dynamics of freely moving charge carriers is the one providing the main contribution to the background absorption. The IRAV modes, probing a different subset of charges, represent a charge carrier species that undergo a slower, effectively monomolecular, recombination process. Their sensitivity toward structural changes implies that the IRAV modes should react to strongly localized charge carriers, in particular, since localization processes directly affect the participating MA cation. The expected lower mobility and increased barrier toward recombination of the localized charges agree with the observed slower, predominantly monomolecular decay of the IRAV signal on a time scale of a few nanoseconds.

The sensitivity of the organic cations toward charges in their vicinity has been a recurring theme in the interpretation of charge-related effects in perovskites,[8,27,28,50] and reorientation of the MA within the inorganic crystal has indeed been shown to occur with a time constant of 3 ps, similar to the initial increase of the IRAV. With the IRAV as an indicator of charges under the influence of localization sites, be they of dynamic or static nature, its rise time of 3 ps can be interpreted as their structural formation time. Considering the slower reaction of the inorganic lead halide lattice, this result is in good agreement with recent time-resolved diffused X-ray scattering measurements which showed polaron formation to occur within the first 20 ps.[51]

In summary, our results indicate that a subgroup of charges undergoes a picosecond localization process. We show that these localized charges are not identical with freely moving charge carriers but seem to participate in joint monomolecular recombination processes. Localization is accompanied by structural deformation involving the methylammonium cations. The associated IRAV modes are shown to be sensitive indicators of the structural distortions and allow for a temporal characterization of this process. Thus, our findings highlight the interplay between structural and electronic properties and demonstrate their influence on charge carrier dynamics relevant for optoelectronic and solar cell applications of hybrid lead halide perovskites.

■ ASSOCIATED CONTENT

Supporting Information

The Supporting Information is available free of charge at https://pubs.acs.org/doi/10.1021/acs.jpclett.1c00935.

Additional details on the estimation of initial charge carrier densities, the nature of the interaction between MA molecules and photoexcited charges, temperature-induced absorption changes and on the fit of the IRAV dynamics; transient spectra at charge carrier densities of 2.7×10 and 5.4×10^{20} cm^{-3} as well as the amplitude of the background absorption signal for different initial carrier densities with a linear fit; data with pump and probe pulses being polarized parallel (PDF)

■ AUTHOR INFORMATION

Corresponding Authors

Cesare Soci − *Energy Research Institute @ NTU (ERI@N), Nanyang Technological University, Singapore 637553; Division of Physics and Applied Physics, School of Physical and Mathematical Sciences, Nanyang Technological*

https://doi.org/10.1021/acs.jpclett.1c00935
J. Phys. Chem. Lett. 2021, 12, 4428−4433

University, Singapore 637371; orcid.org/0000-0002-0149-9128; Email: csoci@ntu.edu.sg

Hristo Iglev – *Physik-Department, Lehrstuhl für Laser- und Röntgenphysik, Technische Universität München, 85748 Garching, Germany;* orcid.org/0000-0001-9208-0068; Email: higlev@ph.tum.de

Authors

Klara Stallhofer – *Physik-Department, Lehrstuhl für Laser- und Röntgenphysik, Technische Universität München, 85748 Garching, Germany;* orcid.org/0000-0001-6314-0156

Matthias Nuber – *Physik-Department, Lehrstuhl für Laser- und Röntgenphysik, Technische Universität München, 85748 Garching, Germany;* orcid.org/0000-0002-4409-3590

Daniele Cortecchia – *Interdisciplinary Graduate School, Nanyang Technological University, Singapore 639798; Energy Research Institute @ NTU (ERI@N), Nanyang Technological University, Singapore 637553;* orcid.org/0000-0001-8623-9191

Annalisa Bruno – *Energy Research Institute @ NTU (ERI@N), Nanyang Technological University, Singapore 637553;* orcid.org/0000-0002-6963-1682

Reinhard Kienberger – *Physik-Department, Lehrstuhl für Laser- und Röntgenphysik, Technische Universität München, 85748 Garching, Germany*

Felix Deschler – *Physik-Department, Walter Schottky Institut, Technische Universität München, 85748 Garching, Germany;* orcid.org/0000-0002-0771-3324

Complete contact information is available at: https://pubs.acs.org/10.1021/acs.jpclett.1c00935

Notes

The authors declare no competing financial interest.

■ ACKNOWLEDGMENTS

This research was supported by the Deutsche Forschungsgemeinschaft (DFG) via the Clusters of Excellence "Munich-Centre of Advanced Photonics (MAP)" and "e-conversion" EXC 2089/1-390776260, by the Singapore National Research Foundation under the Energy Innovation Research Program (CRP Award NRF-CRP14-2014-03 and Solar CRP: S18-1176-SCRP), and by the A*STAR-AME programmatic grant (Grant A18A7b0058). M.N. thanks the "Studienstiftung des deutschen Volkes" for a PhD scholarship.

■ REFERENCES

(1) Vaynzof, Y. The future of perovskite photovoltaics—Thermal evaporation or solution processing? *Adv. Energy Mater.* **2020**, *10*, 2003073.

(2) Li, J.; Dewi, H. A.; Wang, H.; Lew, J. H.; Mathews, N.; Mhaisalkar, S.; Bruno, A. Design of perovskite thermally co-evaporated highly efficient mini-modules with high geometrical fill factors. *Sol. RRL* **2020**, *4*, 2000473.

(3) Li, J.; Wang, H.; Chin, X. Y.; Dewi, H. A.; Vergeer, K.; Goh, T. W.; Lim, J. W. M.; Lew, J. H.; Loh, K. P.; Soci, C.; et al. Highly efficient thermally co-evaporated perovskite solar cells and mini-modules. *Joule* **2020**, *4*, 1035–1053.

(4) Egger, D. A.; Bera, A.; Cahen, D.; Hodes, G.; Kirchartz, T.; Kronik, L.; Lovrincic, R.; Rappe, A. M.; Reichman, D. R.; Yaffe, O. What remains unexplained about the properties of halide perovskites? *Adv. Mater.* **2018**, *30*, No. e1800691.

(5) Alarousu, E.; El-Zohry, A. M.; Yin, J.; Zhumekenov, A. A.; Yang, C.; Alhabshi, E.; Gereige, I.; AlSaggaf, A.; Malko, A. V.; Bakr, O. M.; et al. Ultralong radiative states in hybrid perovskite crystals: compositions for submillimeter diffusion lengths. *J. Phys. Chem. Lett.* **2017**, *8*, 4386–4390.

(6) Niesner, D.; Zhu, H.; Miyata, K.; Joshi, P. P.; Evans, T. J. S.; Kudisch, B. J.; Trinh, M. T.; Marks, M.; Zhu, X.-Y. Persistent energetic electrons in methylammonium lead iodide perovskite thin films. *J. Am. Chem. Soc.* **2016**, *138*, 15717–15726.

(7) Zhu, X.-Y.; Podzorov, V. Charge carriers in hybrid organic-inorganic lead halide perovskites might be protected as large polarons. *J. Phys. Chem. Lett.* **2015**, *6*, 4758–4761.

(8) Zhu, H.; Miyata, K.; Fu, Y.; Wang, J.; Joshi, P. P.; Niesner, D.; Williams, K. W.; Jin, S.; Zhu, X.-Y. Screening in crystalline liquids protects energetic carriers in hybrid perovskites. *Science* **2016**, *353*, 1409–1413.

(9) Miyata, K.; Meggiolaro, D.; Trinh, M. T.; Joshi, P. P.; Mosconi, E.; Jones, S. C.; De Angelis, F.; Zhu, X.-Y. Large polarons in lead halide perovskites. *Sci. Adv.* **2017**, *3*, No. e1701217.

(10) Brennan, M. C.; Ruth, A.; Kamat, P. V.; Kuno, M. Photoinduced anion segregation in mixed halide perovskites. *Trends in Chemistry* **2020**, *2*, 282–301.

(11) Chen, T.; Chen, W.-L.; Foley, B. J.; Lee, J.; Ruff, J. P. C.; Ko, J. Y. P.; Brown, C. M.; Harriger, L. W.; Zhang, D.; Park, C.; et al. Origin of long lifetime of band-edge charge carriers in organic-inorganic lead iodide perovskites. *Proc. Natl. Acad. Sci. U. S. A.* **2017**, *114*, 7519–7524.

(12) Anusca, I.; Balčiūnas, S.; Gemeiner, P.; Svirskas, Š.; Sanlialp, M.; Lackner, G.; Fettkenhauer, C.; Belovickis, J.; Samulionis, V.; Ivanov, M.; et al. Dielectric response: answer to many questions in the methylammonium lead halide solar cell absorbers. *Adv. Energy Mater.* **2017**, *7*, 1700600.

(13) Gallop, N. P.; Selig, O.; Giubertoni, G.; Bakker, H. J.; Rezus, Y. L. A.; Frost, J. M.; Jansen, T. L. C.; Lovrincic, R.; Bakulin, A. A. Rotational cation dynamics in metal halide perovskites: effect on phonons and material properties. *J. Phys. Chem. Lett.* **2018**, *9*, 5987–5997.

(14) Munson, K. T.; Swartzfager, J. R.; Gan, J.; Asbury, J. B. Does dipolar motion of organic cations affect polaron dynamics and bimolecular recombination in halide perovskites? *J. Phys. Chem. Lett.* **2020**, *11*, 3166–3172.

(15) Zhu, H.; Trinh, M. T.; Wang, J.; Fu, Y.; Joshi, P. P.; Miyata, K.; Jin, S.; Zhu, X.-Y. Organic cations might not be essential to the remarkable properties of band edge carriers in lead halide perovskites. *Adv. Mater.* **2017**, *29*, 1603072.

(16) Motta, C.; El-Mellouhi, F.; Kais, S.; Tabet, N.; Alharbi, F.; Sanvito, S. Revealing the role of organic cations in hybrid halide perovskite $CH_3NH_3PbI_3$. *Nat. Commun.* **2015**, *6*, 7026.

(17) Narra, S.; Chung, C.-C.; Diau, E. W.-G.; Shigeto, S. Simultaneous observation of an intraband transition and distinct transient species in the infrared region for perovskite solar cells. *J. Phys. Chem. Lett.* **2016**, *7*, 2450–2455.

(18) Taylor, V. C. A.; Tiwari, D.; Duchi, M.; Donaldson, P. M.; Clark, I. P.; Fermin, D. J.; Oliver, T. A. A. Investigating the role of the organic cation in formamidinium lead iodide perovskite using ultrafast spectroscopy. *J. Phys. Chem. Lett.* **2018**, *9*, 895–901.

(19) Munson, K. T.; Grieco, C.; Kennehan, E. R.; Stewart, R. J.; Asbury, J. B. Time-resolved infrared spectroscopy directly probes free and trapped carriers in organo-halide perovskites. *ACS Energy Lett.* **2017**, *2*, 651–658.

(20) Munson, K. T.; Kennehan, E. R.; Doucette, G. S.; Asbury, J. B. Dynamic disorder dominates delocalization, transport, and recombination in halide perovskites. *Chem.* **2018**, *4*, 2826–2843.

(21) Munson, K. T.; Doucette, G. S.; Kennehan, E. R.; Swartzfager, J. R.; Asbury, J. B. Vibrational probe of the structural origins of slow recombination in halide perovskites. *J. Phys. Chem. C* **2019**, *123*, 7061–7073.

(22) Ehrenfreund, E.; Vardeny, Z.; Brafman, O.; Horovitz, B. Amplitude and phase modes in trans-polyacetylene: resonant raman scattering and induced infrared activity. *Phys. Rev. B: Condens. Matter Mater. Phys.* **1987**, *36*, 1535–1553.

(23) Zamadar, M.; Asaoka, S.; Grills, D. C.; Miller, J. R. Giant infrared absorption bands of electrons and holes in conjugated molecules. *Nat. Commun.* **2013**, *4*, 2818.
(24) Anderson, M.; Ramanan, C.; Fontanesi, C.; Frick, A.; Surana, S.; Cheyns, D.; Furno, M.; Keller, T.; Allard, S.; Scherf, U.; et al. Displacement of polarons by vibrational modes in doped conjugated polymers. *Phys. Rev. Mater.* **2017**, *1*, 55604.
(25) Wong, W. P. D.; Yin, J.; Chaudhary, B.; Chin, X. Y.; Cortecchia, D.; Lo, S.-Z. A.; Grimsdale, A. C.; Mohammed, O. F.; Lanzani, G.; Soci, C. Large polaron self-trapped states in three-dimensional metal-halide perovskites. *ACS Materials Lett.* **2020**, *2*, 20−27.
(26) Ambrosio, F.; Meggiolaro, D.; Mosconi, E.; De Angelis, F. Charge localization, stabilization, and hopping in lead halide perovskites: competition between polaron stabilization and cation disorder. *ACS Energy Lett.* **2019**, *4*, 2013−2020.
(27) Ma, J.; Wang, L.-W. Nanoscale charge localization induced by random orientations of organic molecules in hybrid perovskite $CH_3NH_3PbI_3$. *Nano Lett.* **2015**, *15*, 248−253.
(28) Zhang, Z.; Long, R.; Tokina, M. V.; Prezhdo, O. V. Interplay between localized and free charge carriers can explain hot fluorescence in the CH3NH3PbBr3 perovskite: time-domain ab initio analysis. *J. Am. Chem. Soc.* **2017**, *139*, 17327−17333.
(29) Uratani, H.; Chou, C.-P.; Nakai, H. Quantum mechanical molecular dynamics simulations of polaron formation in methylammonium lead iodide perovskite. *Phys. Chem. Chem. Phys.* **2020**, *22*, 97−106.
(30) Yaffe, O.; Guo, Y.; Tan, L. Z.; Egger, D. A.; Hull, T.; Stoumpos, C. C.; Zheng, F.; Heinz, T. F.; Kronik, L.; Kanatzidis, M. G.; et al. Local polar fluctuations in lead halide perovskite crystals. *Phys. Rev. Lett.* **2017**, *118*, 136001.
(31) Wu, X.; Tan, L. Z.; Shen, X.; Hu, T.; Miyata, K.; Trinh, M. T.; Li, R.; Coffee, R.; Liu, S.; Egger, D. A.; et al. Light-induced picosecond rotational disordering of the inorganic sublattice in hybrid perovskites. *Science Advances* **2017**, *3*, No. e1602388.
(32) Rivett, J. P. H.; Tan, L. Z.; Price, M. B.; Bourelle, S. A.; Davis, N. J. L. K.; Xiao, J.; Zou, Y.; Middleton, R.; Sun, B.; Rappe, A. M.; et al. Long-lived polarization memory in the electronic states of lead-halide perovskites from local structural dynamics. *Nat. Commun.* **2018**, *9*, 3531.
(33) Emin, D. *Optical Properties of Large and Small Polarons and Bipolarons*, 1993.
(34) Stallhofer, K.; Nuber, M.; Kienberger, R.; Körstgens, V.; Müller-Buschbaum, P.; Iglev, H. Dynamics of short-lived polaron pairs and polarons in polythiophene derivatives observed via infrared-activated vibrations. *J. Phys. Chem. C* **2019**, *123*, 28100−28105.
(35) Yin, J.; Wang, Z.; Fazzi, D.; Shen, Z.; Soci, C. First-principles study of the nuclear dynamics of doped conjugated polymers. *J. Phys. Chem. C* **2016**, *120*, 1994−2001.
(36) Boxer, S. G. Stark realities. *J. Phys. Chem. B* **2009**, *113*, 2972−2983.
(37) Schuck, G.; Többens, D. M.; Koch-Müller, M.; Efthimiopoulos, I.; Schorr, S. Infrared Spectroscopic Study of Vibrational Modes across the Orthorhombic−Tetragonal Phase Transition in Methylammonium Lead Halide Single Crystals. *J. Phys. Chem. C* **2018**, *122*, 5227−5237.
(38) Patel, J. B.; Milot, R. L.; Wright, A. D.; Herz, L. M.; Johnston, M. B. Formation dynamics of $CH_3NH_3PbI_3$ perovskite following two-step layer deposition. *J. Phys. Chem. Lett.* **2016**, *7*, 96−102.
(39) Yin, T.; Fang, Y.; Fan, X.; Zhang, B.; Kuo, J.-L.; White, T. J.; Chow, G. M.; Yan, J.; Shen, Z. X. Hydrogen-Bonding Evolution during the Polymorphic Transformations in $CH_3NH_3PbBr_3$: Experiment and Theory. *Chem. Mater.* **2017**, *29*, 5974−5981.
(40) Badger, R. M. A relation between internuclear distances and bond force constants. *J. Chem. Phys.* **1934**, *2*, 128−131.
(41) Kendrick, W. J.; Jirásek, M.; Peeks, M. D.; Greetham, G. M.; Sazanovich, I. V.; Donaldson, P. M.; Towrie, M.; Parker, A. W.; Anderson, H. L. Mechanisms of IR amplification in radical cation polarons. *Chem. Sci.* **2020**, *11*, 2112−2120.
(42) Herz, L. M. Charge-Carrier Dynamics in Organic-Inorganic Metal Halide Perovskites. *Annu. Rev. Phys. Chem.* **2016**, *67*, 65−89.
(43) deQuilettes, D. W.; Frohna, K.; Emin, D.; Kirchartz, T.; Bulovic, V.; Ginger, D. S.; Stranks, S. D. Charge-carrier recombination in halide perovskites. *Chem. Rev.* **2019**, *119*, 11007−11019.
(44) Savenije, T. J.; Ponseca, C. S.; Kunneman, L.; Abdellah, M.; Zheng, K.; Tian, Y.; Zhu, Q.; Canton, S. E.; Scheblykin, I. G.; Pullerits, T.; et al. Thermally Activated Exciton Dissociation and Recombination Control the Carrier Dynamics in Organometal Halide Perovskite. *J. Phys. Chem. Lett.* **2014**, *5*, 2189−2194.
(45) Yang, Y.; Yang, M.; Li, Z.; Crisp, R.; Zhu, K.; Beard, M. C. Comparison of Recombination Dynamics in $CH_3NH_3PbBr_3$ and $CH_3NH_3PbI_3$ Perovskite Films: Influence of Exciton Binding Energy. *J. Phys. Chem. Lett.* **2015**, *6*, 4688−4692.
(46) Johnston, M. B.; Herz, L. M. Hybrid perovskites for photovoltaics: charge-carrier recombination, diffusion, and radiative efficiencies. *Acc. Chem. Res.* **2016**, *49*, 146−154.
(47) Richter, J. M.; Abdi-Jalebi, M.; Sadhanala, A.; Tabachnyk, M.; Rivett, J. P. H.; Pazos-Outón, L. M.; Gödel, K. C.; Price, M.; Deschler, F.; Friend, R. H. Enhancing photoluminescence yields in lead halide perovskites by photon recycling and light out-coupling. *Nat. Commun.* **2016**, *7*, 13941.
(48) Davies, C. L.; Filip, M. R.; Patel, J. B.; Crothers, T. W.; Verdi, C.; Wright, A. D.; Milot, R. L.; Giustino, F.; Johnston, M. B.; Herz, L. M. Bimolecular recombination in methylammonium lead triiodide perovskite is an inverse absorption process. *Nat. Commun.* **2018**, *9*, 293.
(49) Srimath Kandada, A. R.; Neutzner, S.; D'Innocenzo, V.; Tassone, F.; Gandini, M.; Akkerman, Q. A.; Prato, M.; Manna, L.; Petrozza, A.; Lanzani, G. Nonlinear carrier interactions in lead halide perovskites and the role of defects. *J. Am. Chem. Soc.* **2016**, *138*, 13604−13611.
(50) Neukirch, A. J.; Nie, W.; Blancon, J.-C.; Appavoo, K.; Tsai, H.; Sfeir, M. Y.; Katan, C.; Pedesseau, L.; Even, J.; Crochet, J. J.; et al. Polaron Stabilization by Cooperative Lattice Distortion and Cation Rotations in Hybrid Perovskite Materials. *Nano Lett.* **2016**, *16*, 3809−3816.
(51) Guzelturk, B.; Winkler, T.; van de Goor, T. W. J.; Smith, M. D.; Bourelle, S. A.; Feldmann, S.; Trigo, M.; Teitelbaum, S. W.; Steinrück, H.-G.; La Pena, G. A. de; et al. Visualization of dynamic polaronic strain fields in hybrid lead halide perovskites. *Nat. Mater.* **2021**, *20*, 618.

https://doi.org/10.1021/acs.jpclett.1c00935
J. Phys. Chem. Lett. 2021, 12, 4428−4433